



Strain induced martensitic transformations in two austenitic stainless steels : macro-micro behaviour

Stéphanie Nanga, André Pineau, Pierre-Olivier Santacreu, Benoit Tanguy

► To cite this version:

Stéphanie Nanga, André Pineau, Pierre-Olivier Santacreu, Benoit Tanguy. Strain induced martensitic transformations in two austenitic stainless steels : macro-micro behaviour. ECF 17, Sep 2008, Brno, Czech Republic. pp.1373-1380. ⟨hal-00329766⟩

HAL Id: hal-00329766

<https://hal.science/hal-00329766v1>

Submitted on 5 Jun 2013

HAL is a multi-disciplinary open access archive for the deposit and dissemination of scientific research documents, whether they are published or not. The documents may come from teaching and research institutions in France or abroad, or from public or private research centers.

L'archive ouverte pluridisciplinaire **HAL**, est destinée au dépôt et à la diffusion de documents scientifiques de niveau recherche, publiés ou non, émanant des établissements d'enseignement et de recherche français ou étrangers, des laboratoires publics ou privés.



HAL Authorization

Strain Induced Martensitic Transformations in two Austenitic Stainless Steels: Macro-Micro Behaviour

S. Nanga¹, A. Pineau^{1*}, B. Tanguy² and P.-O. Santacreu³

¹ Centre des matériaux, Ecole des Mines de Paris UMR CNRS 7633, BP 87, F-91003 Evry cedex, France

² Centre d'Etudes Nucléaires - Site de Saclay, F-91191 Gif sur Yvette Cedex, France

³ ArcelorMittal Isbergues R & D, BP 15, 62330 Isbergues, France

*andre.pineau@ensmp.fr

Keywords: stainless steels, martensite transformation, strain rate, stress state, strain path.

Abstract. Two grades of austenitic stainless steels, AISI 301LN and AISI 201, were monotonically tested under uniaxial tension, shear and deep drawing over a wide temperature range [-150°C; +150°C] and a wide strain rate range [$3 \cdot 10^{-4} \text{ s}^{-1}$; 200 s^{-1}]. Non monotonic loadings were also performed to study the strain path dependence on phase transformation, mechanical behaviour and microstructures. TEM examinations were used for microstructural observations and SEM for fractographic analysis. Correlations between transformations micromechanisms and macroscopic properties were established.

Introduction

Good corrosion resistance, high strength and ductility are the characteristics that give to austenitic stainless steels their interest for automotive part applications. These characteristics are partly due to the ability of such materials to transform from the initial face-centered-cubic austenite (γ) to body-centered-cubic (α') or hexagonal-compact (ϵ) martensite upon plastic deformation; this is referred to strain-induced martensite. This transformation occurs in-between the temperature M_s , which is the martensite start temperature and M_d , the temperature above which no phase transformation occurs by plastic deformation. The alloy composition has a direct effect on the austenite stability. Angel [1] was the first author to study the influence of composition on the $\gamma \rightarrow \alpha'$ transformation. He introduced the concept of M_{d30} , the temperature at which 50% of martensite is formed by the application of 0.3 tensile strain. The strong effect of C and N was established and confirmed by the work of Eichelman and Hull [2]. These authors also established the impact of Cr and Ni, which is slighter than C and N influence.

The $\gamma \rightarrow \alpha'$ transformation mechanism is believed to result from shear bands intersections [3,4]. The nucleation sites can be stacking fault bundles intersections, slip bands and grain or twin boundaries intersections [4-7]. Blanc et al. [8] have established two sequences: $\gamma \rightarrow \epsilon \rightarrow \alpha'$ and $\gamma \rightarrow \alpha'$. As planar glide is the key factor, the related stacking fault energy (SFE) also has a critical role in the strain induced martensite formation, as shown by Lecroisey and Pineau [4], then by Olson and Cohen [9]. These authors have proposed a physical-based kinetics model for the strain induced $\gamma \rightarrow \alpha'$ transformation.

Besides temperature, composition effect and SFE, strain rate and strain path are variables that must be taken into account for a full description of transformation phenomena. Strain rates ranging from $3 \cdot 10^{-4} \text{ s}^{-1}$ to 400 s^{-1} were explored and number of authors (see e.g. [7,13]) found that, due to adiabatic heating, the amount of martensite phase formed during a tensile test decreases as

compared to quasi-static tests, and hence strongly affects the mechanical properties. Hecker et al [10] found that in 304, more martensite was formed during biaxial tension than during pure tension. The aims of the present study devoted to two grades of austenitic stainless steels, 201 and 301LN, were: (i) to provide the inputs necessary to model the kinetics of the $\gamma \rightarrow \alpha'$ strain-induced phase transformation under a wide range of temperature, strain rate and stress triaxiality ratio, (ii) to investigate the effect of non radial loading on the $\gamma \rightarrow \alpha'$ transformation and (iii) to relate quantitatively the phase transformation and the mechanical properties.

Experimental procedures

The materials were provided by Ugine&Alz in sheet form of 1.5 mm thickness. They were cold-rolled then annealed. Grade 301LN was afterwards subjected to a skin-pass process. The investigated steels composition is given table 1.

Table 1: chemical composition of grades AISI 301LN and AISI 201 in weight percent.

	%C	%N	%Cr	%Ni	%Mn	%Si	%Mo	%Nb	%Ti	%Cu	%P	%S
AISI 301LN	0.024	0.122	17.470	6.556	1.227	0.565	0.199	0.002	0.001	0.172	0.031	0.006
AISI 201	0.090	0.165	16.268	4.120	6.463	0.503	0.145	0.000	0.000	0.000	0.030	0.001

Quasi-static tensile specimens were taken perpendicular to the rolling direction and tested to fracture from -150°C to 150°C at 3.10^{-4} s^{-1} strain rate. Higher strain rates were applied using a dedicated tensile machine for very high speed tests. For high speed tests, the load was followed using a 65 kN capacity Kistler and strain, with a laser extensometer using Doppler effect.

To change the strain state, simple shear tests were also performed on grade 301LN. Plane strain and balanced biaxial tension conditions also were achieved by performing deep drawing tests at room temperature.

The α' martensite formation was investigated using saturation magnetic measurements on interrupted test specimens.

Scanning and transmission electron microscopy were used to follow the evolution of the deformation microstructures.

Results and Discussion

Temperature and strain rate effects. Tensile curves obtained at 3.10^{-4} s^{-1} strain rate and at various temperatures for both grades are presented on Fig.1 and Fig.2. One can see the inflexion taken by the curves when $\gamma \rightarrow \alpha'$ transformation occurs. If the stress-strain curves are quite similar, grade 301LN undergoes a martensitic transformation in a greater extent than grade 201. This is confirmed by the kinetics of martensite formation. Md temperature is around 80°C for grade 301LN and 60°C for grade 201. The uniform elongation evolution with temperature variation is shown in Fig.3. A ductility peak is observed around Md temperature. The energy stored during tensile tests, measured by the surface under the stress-strain curves, was calculated and is reported in Fig.4. Grade 201 shows a better ability to absorb energy and a higher uniform elongation. The fact that this grade shows less transformation implies that there is another mechanism to explain its mechanical behaviour.

The isothermal kinetics of $\gamma \rightarrow \alpha'$ phase transformation was modelled using the law proposed by Olson and Cohen [9]:

$$f_{\alpha'} = 1 - \exp[-\beta(T) \times (1 - \exp(-\alpha(T) \times \epsilon))^{4.5}]. \quad (1)$$

The parameters $\alpha(T)$ and $\beta(T)$ were deduced from the data obtained at various temperatures.

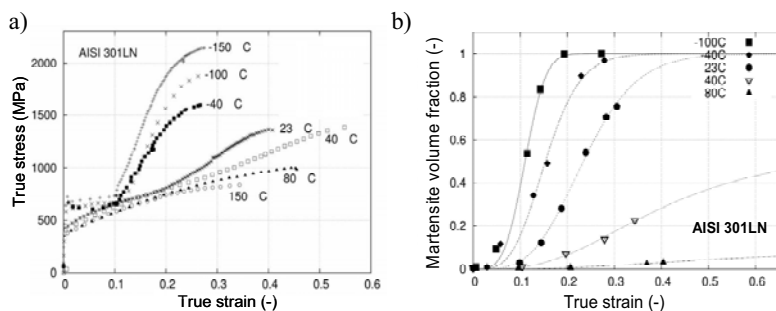


Fig.1: Temperature effect on martensitic transformation on austenitic steels 301LN; a) quasi-static uniaxial tensile curves at 3.10-4 s-1 strain rate; b) corresponding transformation kinetics.

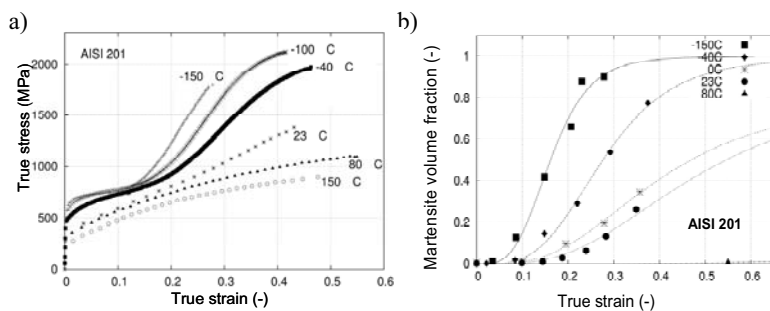


Fig.2: Temperature effect on martensitic transformation on austenitic steels 201; a) quasi-static uniaxial tensile curves at 3.10-4 s-1 strain rate; b) corresponding transformation kinetics.

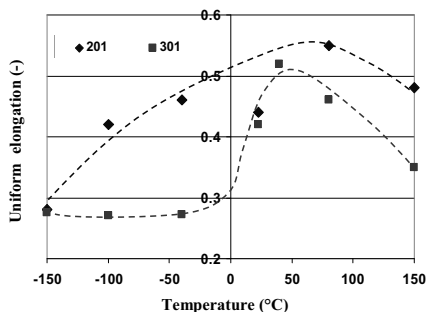


Fig.3: Temperature evolution of uniform elongation; a peak is observed around Md temperature.

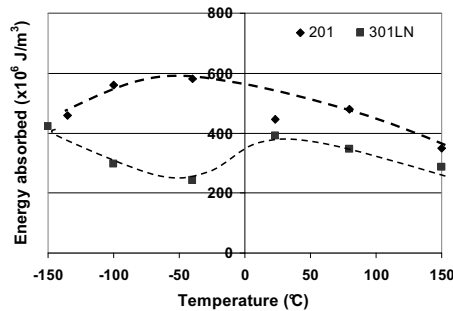


Fig.4: Temperature evolution of the energy absorbed; grade 201 has greater absorption ability.

The results of TEM observations on specimens deformed by various amounts and at two temperatures are summarized in Fig. 5. The sequence $\gamma \rightarrow \epsilon \rightarrow \alpha'$ is observed on grade 201, while the direct $\gamma \rightarrow \alpha'$ transformation occurs in 301LN steel. Detailed observations showed that the nuclei of α' martensite were located at planar defects intersections (stacking faults, twins, ϵ platelets). It should be noticed that in 201 steel the interactions between planar defects play a very significant role in explaining the mechanical behaviour of this material which is more stable than 301LN steel.

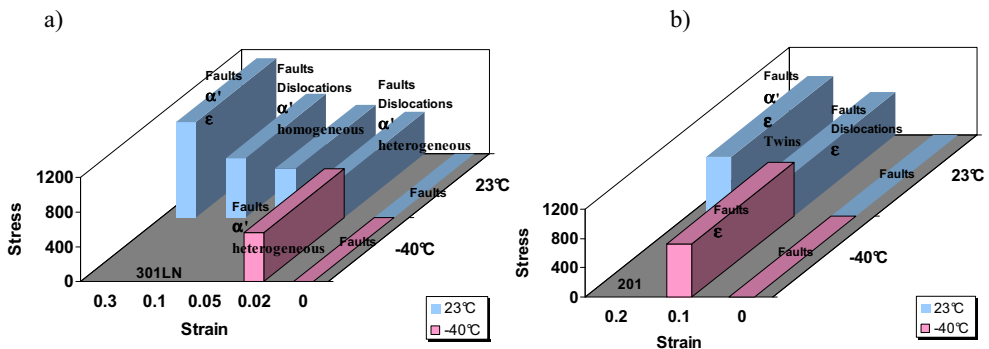


Fig.5: Deformation and transformation microstructures observed by TEM with transformation sequence obtained at -40°C and 23°C for a) grade 301LN and b) grade 201.

SEM observations showed that in all cases, ductile fracture occurs by dimple formation (Fig. 6). A larger amount of inclusions were found in 301LN steel as compared to 201. This explains why 301LN steel exhibits a lower strain to fracture.

The stress-strain curves obtained at a strain rate of 50 s^{-1} at room temperature are presented in Fig.7. The inflexion previously observed for quasi-static loading disappears and the related transformation kinetics curves show a decrease in martensite amount. The yield strength is considerably increased and no loss of ductility is observed. Ferreira et al [11] established that high strain rates promote the formation of stacking faults and mechanical twins. It is also expected that ϵ -martensite formation is enhanced by high strain rates at the expense of α' -martensite. Therefore, the mechanical behaviour results from two competing effects. The increase in strain rate promotes planar slip character with the formation of planar defects. This provides a strengthening effect. Strain rate increase also provokes an elevation of temperature which produces a weakening effect largely associated with α' martensite reduction.

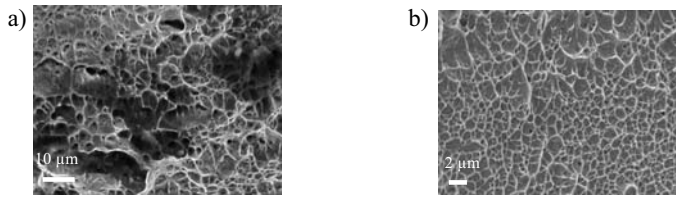


Fig. 6: SEM observations of tensile specimen after fracture at room temperature of a) grade 301LN with many inclusions and b) grade 201. The same observations were made for all temperatures.

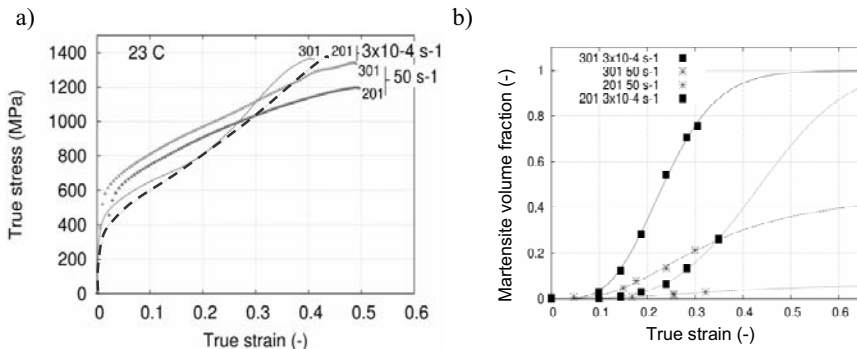


Fig.7: Strain effect on a) stress-strain curves at 50 s⁻¹ strain rate and b) associated transformation kinetics.

The non isothermal value for the amount of α' martensite for steel 301LN was calculated using the Olson and Cohen law, integrated along the stress-strain curve and using the results of temperature measurements. The kinetics obtained is compared to experimental results at 50 s⁻¹. Prediction underestimates the martensite volume fraction at 23°C (Fig. 8a). That is, if adiabatic effect induces a decrease of martensite amount, strain rate, on the contrary, has a positive effect on the transformation. On the other side, testing at an initial temperature of -40°C, when heating lies in the range [Ms, Md], it is shown on Fig.8b that counting only for adiabatic effect is sufficient to predict the volume fraction curve. It appears therefore that the kinetics of $\gamma \rightarrow \alpha'$ transformation observed at high strain rate are very much dependent of the position of the initial test temperature compared to Md temperature.

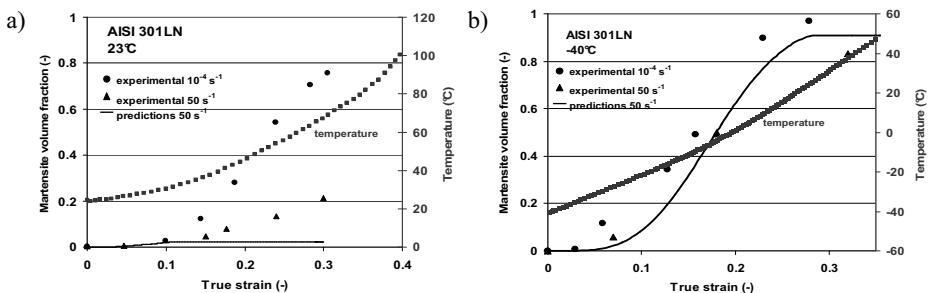


Fig.8: Martensitic transformation kinetics during high speed testing a) at room temperature, prediction underestimates the experimental volume fraction; b) at -40°C, prediction approaches the experimental values.

Stress state effects. The results of α' measurements obtained under balanced biaxial tension, plane strain, uniaxial tension and simple shear are given in Fig.9. The stress triaxiality ratio ($\tau = \sigma_m / \sigma_{eq}$, where σ_m is the hydrostatic stress and σ_{eq} the von Mises equivalent stress) corresponding to these loading conditions are 0.66, 0.57, 0.33 and 0, respectively. From the literature [12-14], it is expected that for a given applied strain, the amount of α' martensite increases with τ . Figure 9 shows that the martensite volume fraction is maximum for balanced biaxial tension and uniaxial tension. This is to some extent contradictory to expected results. Similar data have been published by Diani and Parks [15]. The explanation arises considering how martensite is nucleated. Indeed, the shear band intersection evolution with strain may be different for uniaxial tension and plane strain state. Then at microscopic scale, not only should the triaxiality parameter be taken into account, but also the strain state.

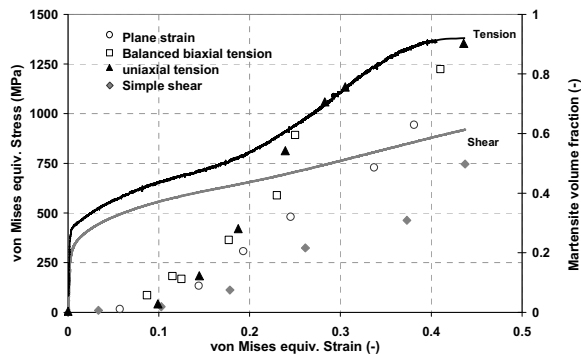


Fig.9: Stress state effect on transformation; plane strain curve is lower than uniaxial tension curve.

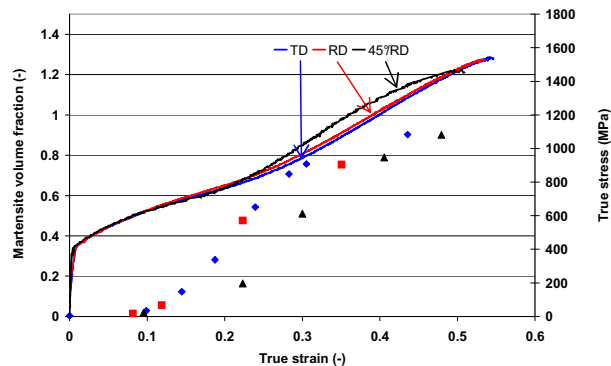


Fig.10: Anisotropic effect on transformation marked for 45° orientation.

Strain path effects. X-ray diffraction measurements showed that the materials were quasi-isotropic. However the mechanical response obtained in uniaxial tension for specimens sampled along rolling direction RD, perpendicular to the rolling direction TD and at 45° from RD (Fig.10), shows a significant difference for the specimen oriented at 45°/RD. Transformation kinetics are comparable for RD and TD direction whereas the transformation rate is lower for the 45° oriented specimens, opposite to the trend shown by the mechanical response. The nucleation sites appear to

be more favorable for the RD and TD orientations than at 45° . These tests show that the mechanical behaviour of unstable stainless steels cannot only be explained in terms of α' volume fraction. The loading path influence was investigated by testing tensile specimen of both grades following the sketch shown on Fig.11. Large specimens were firstly predeformed along TD by various amounts. Then smaller specimens were cut along 45° /RD and tested. In this study all specimens were given a total strain of about 0.35. The martensite amount was then measured and the results are presented in Fig.12. When changing the strain path, the extent of martensite amount formed was dependent of the applied pre-strain. For lower pre-strain values ($\epsilon = 0.14$ and $\epsilon = 0.23$), the new kinetics after an orientation change follows the one obtained without pre-strain for the given orientation (Fig.12b). When all nucleation sites have been exhausted ($\epsilon = 0.28$), the kinetics follows the TD orientation curve (Fig.12b).

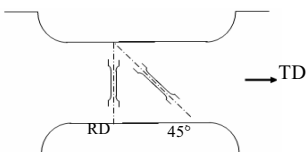


Fig.11: Sampling of tensile specimens pre-strain along transverse direction and tested following two different paths.

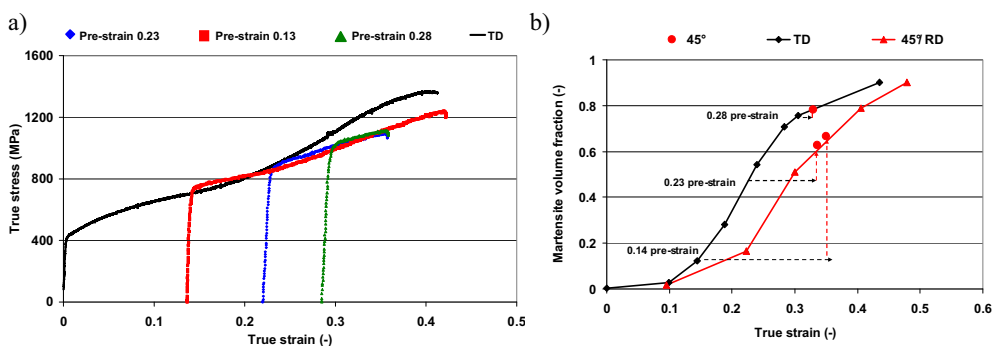


Fig.12: a) Loading path influence on stress-strain curves after 45° orientation change and b) volume fraction measurement after total strain of nearly 0.35.

Summary

- $\gamma \rightarrow \alpha'$ martensitic transformation strongly influences the mechanical response of unstable stainless steel 301LN. The transformation mode $\gamma \rightarrow \epsilon \rightarrow \alpha'$ presented by the more stable grade 201 plays a key role in the mechanical reinforcement mechanism of this material.
- It is suggested that high strain rates promote the ϵ -martensite formation with an increase of flow stress and no loss of ductility. The amount of α' martensite produced at high strain rate can be predicted from isothermal kinetics measurements provided that the temperature remains in the [Ms, Md] range.
- The study of deformation modes and loading path effects shows that the microscopic strain state of grains undergoing nucleation should be considered towards transformation. Further study is necessary to confirm the hypothesis of preferential shear band formation, by

studying the deformation texture of sample loaded in plane strain state or after a loading path change.

- Microstructural study details the martensite formation sequence for both grades. This should be continued for high strain rate to follow deformation microstructure evolution with strain.

References

- [1] T. Angel: J. Iron Steel Inst. (1954), p. 165
- [2] G. H. Eichelman and F. C. Hull: Trans. A.S.M. Vol. 45 (1953), p. 45
- [3] G. Olson and M. Cohen: J. Less Common Metals Vol. 28 (1972), p. 107
- [4] F. Lecroisey and A. Pineau: Met. Trans. Vol. 3 (1972), p. 387
- [5] P. L. Mangonon and G. Thomas: Met. Trans. Vol. 1 (1970), p. 1577
- [6] L. E. Murr, K. P. Staudhammer and S. S. Hecker: Met. Trans. Vol. 13A (1982), p. 627
- [7] J. A. Lichtenfeld, M. C. Mataya and C. J. Van Tyne: Met. Mater. Trans. Vol. 37 (2006), p. 147
- [8] G. Blanc, R. Tricot and R. Castro: *Transformations Martensitiques dans les Aciers Inoxydables Austenitiques Fe-Cr-Ni* (Technical Report, Centre de recherche Ugine Aciers, France 1973).
- [9] G. Olson and M. Cohen: Met. Trans. Vol. 6 (1975), p. 791
- [10] S. S. Hecker, M. G. Stout, K. P. Staudhammer and J. L. Smith: Met. Trans. Vol. 13 (1982), p. 619
- [11] P. J. Ferreira, J. B. Vande Sande, M. Amaral Fortes and A. Kyrolainen: Met. Mater. Trans. Vol. 35A (2004), p. 3091
- [12] J. Talonen, P. Nenonen, G. Pape and H. Hanninen: Met. Mater. Trans. Vol. 36A (2005), p. 421
- [13] R. G. Stringfellow, D. M. Parks and G. B. Olson: Met. Mater. Trans. Vol. 40 (1992), p. 1703
- [14] M. Radu: *Relation entre la Microstructure et le Comportement Mécanique des Aciers TRIP pour Application Automobile* (PhD Report, ENSMP, France 2005).
- [15] J. M. Diani and D. M. Parks: J. Mech. Phys. Solids Vol. 46 (1998), p. 1613